Supplementary Information

Bio-inspired sustained entrainment in immiscible liquid-liquid systems for collecting floating oil

Ziyang Cheng,[ab] Tao Shen,[a] Shuaizhong Chen,[ab] Cunlong Yu,[ab] Panhai Li,[cd] Qirong Tian,[cd] Chuxin Li,[cd] Lei Jiang[ab] and Zhichao Dong*[abd]

[a]CAS Key Laboratory of Bio-inspired Materials and Interfacial Science, Technical Institute of Physics and Chemistry, Chinese Academy of Sciences, Beijing, 100190, China
[b]School of Future Technology, University of Chinese Academy of Sciences, Beijing, 100049, China
[c]School of Chemistry and Materials Science, University of Science and Technology of China, Hefei, Anhui, 230026, China
[d]Suzhou Institute for Advanced Research, University of Science and Technology of China, Suzhou, Jiangsu, 215123, China
*Correspondence Author: dongzhichao@mail.ipc.ac.cn

Experimental section

Chemicals and materials. PMX-200 silicone oils (PDMS) with viscosity of ~10, ~100, ~350, ~1000, and ~10000 mPa·s were of analytical reagent grade (Dow, USA). Water was deionized from Milli-Q equipment with an 18.2 MΩ·cm resistance. Photosensitive resin (Miniature Resin White Color, GOPRINT, China) and aluminum alloy (AlSi10Mg, AmPro Innovations, China) were used for 3D printing. Crude oil was provided by the Shengli oilfield, China.

Characterization of the tested liquids. The viscosities of silicone oils and crude oil were characterized by a cone-plate viscometer (DV-II+ Pro, Brookfield, USA). The water-oil capillary lengths were attained by a surface analyzer (LSA 100, LAUDA Scientific, Germany) with the pendant drop method. The contact angles shown in Fig. S1 were measured by a contact angle DSA25S (KRUSS, Germany) with liquid droplet volume of 2 μL for Fig. S1(a) and S1(b), and 15 μL for Fig. S1(c).

Bumble bee tongue analysis. Optical images of a bumble bee specimen (purchased from Beijing Jiaying Art Insectarium, China) and detailed views of its hairy tongue were captured using optical (DSX1000, Olympus, Japan) and micro-CT imaging (Skyscan 1272, Bruker, USA). The raw data captured by the micro-CT were then reconstructed into tomographic images with NRecon (Bruker, USA) and postprocessed with CTAn (Bruker, USA). Finally, the images were transformed into a 3D model with the volume rendering software CTVox (Bruker, USA) for characterization.

3D-printed sample design, preparation, and analysis. The mesoscale-structured solid objects were designed with 3ds Max Software (Autodesk) and fabricated with photosensitive resin by a liquid crystal display (LCD) 3D printer (Sonic Mini 8K, Phrozen, China) with *x*-*y*-plane resolution of 22 μm and *z*-axis resolution of 20 μm, and aluminum alloy by a metal laser sintering 3D printer (SP261, AmPro Innovations, China) with the accuracy of ±0.05 mm. Optical image of a 3D-printed mesoscale-structured solid object were captured by DSX1000 (Olympus, Japan). Detailed sample morphology was observed by a scanning electron microscope (SEM) at the acceleration voltage of 15 kV and low vacuum mode (QUANTA FEG 250, FEI, USA). The sample

was mounted on an aluminum stub with copper tape and coated with a thin layer of platinum by an ion sputter at 10 mA for 60 s (MC1000, Hitachi, Japan).

Experimental setup for entrainment and liquid-liquid interface analysis. A solid object is immersed from an upper oil layer into a lower water body to a specific depth (D) in a cuboid glass cup at a constant downward speed (U_{down}) by a motorized vertical mobile device (ESM 301, MARK-10, USA). After reaching the depth D at the time point t_0, the immersion stopped and the object remained stationary for a time t. Then the object was withdrawn at a constant upward speed (U_{up}) by ESM 301. The processes were captured using a high-speed camera (Wave, Freefly Systems, USA) with a lens (AT-X M100 PRO D Macro, Tokina, Japan) at 100 fps (1 fps for Fig 3(f)). The statistical data of the shape of the liquid-liquid interface, as well as the oil film thickness over time, were extracted and analyzed from the videos by an open-source tracking software (Tracker, Open Source Physics).

Floating oil collection. The experiment setup for the demonstration with mechanical arm included a 6-axes mechanical arm (AR3, LAMCHUA, China) to control the motion of the structured object array, a semiconductor chilling plate (TEC1-12706 SR) powered by a DC power supply (IT6834, ITECH, China) at 3 V/1.2 A to manipulate the temperature, and a force sensor (RDF-TC10B, Rld-sensor, China) to measure the mass of the entrained liquid. The array with temperature of approximately 25 ℃ was immersed into the crude oil on water surface and then withdrawn to take up and transfer the oil. The oil entrained by the array was then heated to about 35 ℃ and dripped down. The experiment process with temperature variation was observed by an infrared camera (Blackbird precision, JENOPTIK, Germany) and a camera (D7500, Nikon, Japan). In the demonstration with drone, 4 mesoscale-structured objects were mounted on a drone (Mi Drone Mini-YKFJ01FM, Fimi, China). The collection rate per cycle was the mass of the dripped oil divided by the cross-section area of the alloy array. The clean efficiency was calculated with (1 - water content in the collected oil) × 100%, which was attained by a Karl-Fischer moisture titrator (AKF-V6, HOGON, China).

Supplementary Figures and tables

Fig. S1 Contact angle of (a) water in air, (b) silicone oil in air, and (c) water under silicone oil. The silicone oil is of 10 mPa·s, and the substrate is the 3D-printed resin sample used in the experiments in Fig. 1, 2 and 3. The data are shown as mean ± SD (N = 3).

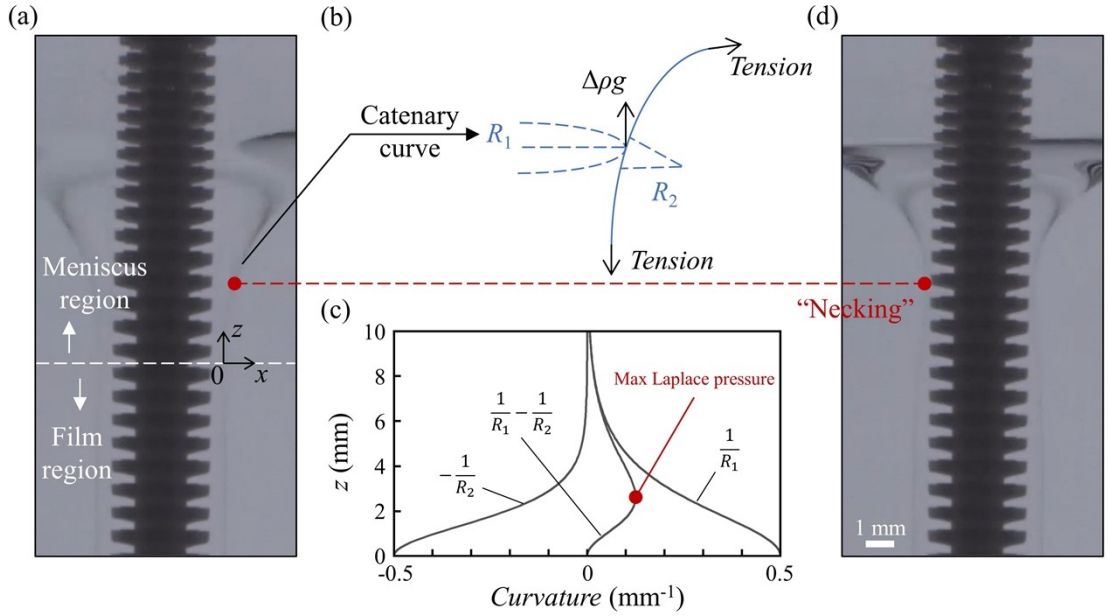

Fig. S2 (a) Initial shape of the interface between water and entrained oil film. According to the its shape in the vertical section view, the interface curve can be divided into the meniscus region of millimetric to centimetric scale and the film region below. The coordinate origin here is set at the boundary of the regions. (b) Schematic of the catenary curve model. (c) Calculated evolution of the principal curvatures of the interface along *z*-axis in the meniscus region. (d) "Necking" behavior that happens in the meniscus region.

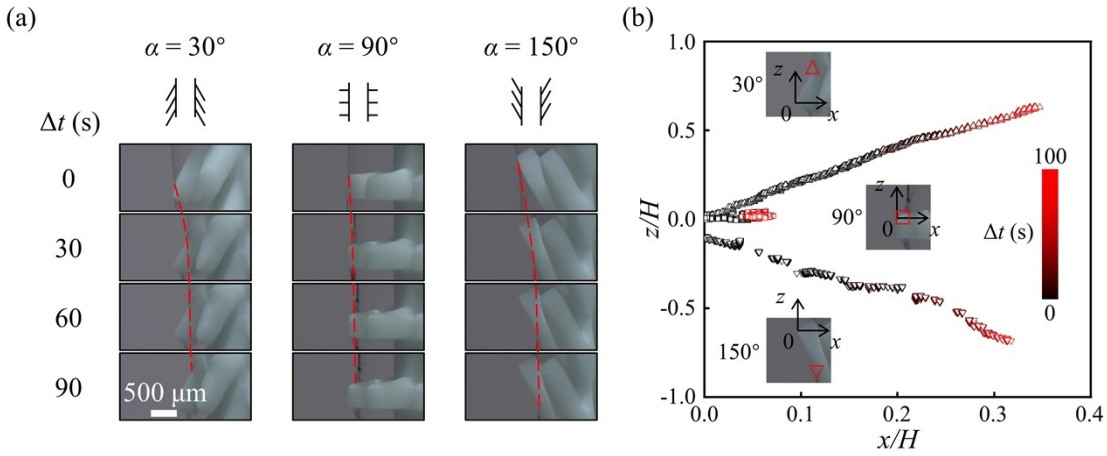

Fig. S3 (a) Optical time sequences and (b) image tracking of the motion of the contact point of the liquid-liquid interface and the solid object with varied unit angle α. We set $\Delta t = 0$ when the liquid-liquid interface is initially observed to contact with the object. And the coordinate origin here is set at the initial contact point at $\Delta t = 0$.

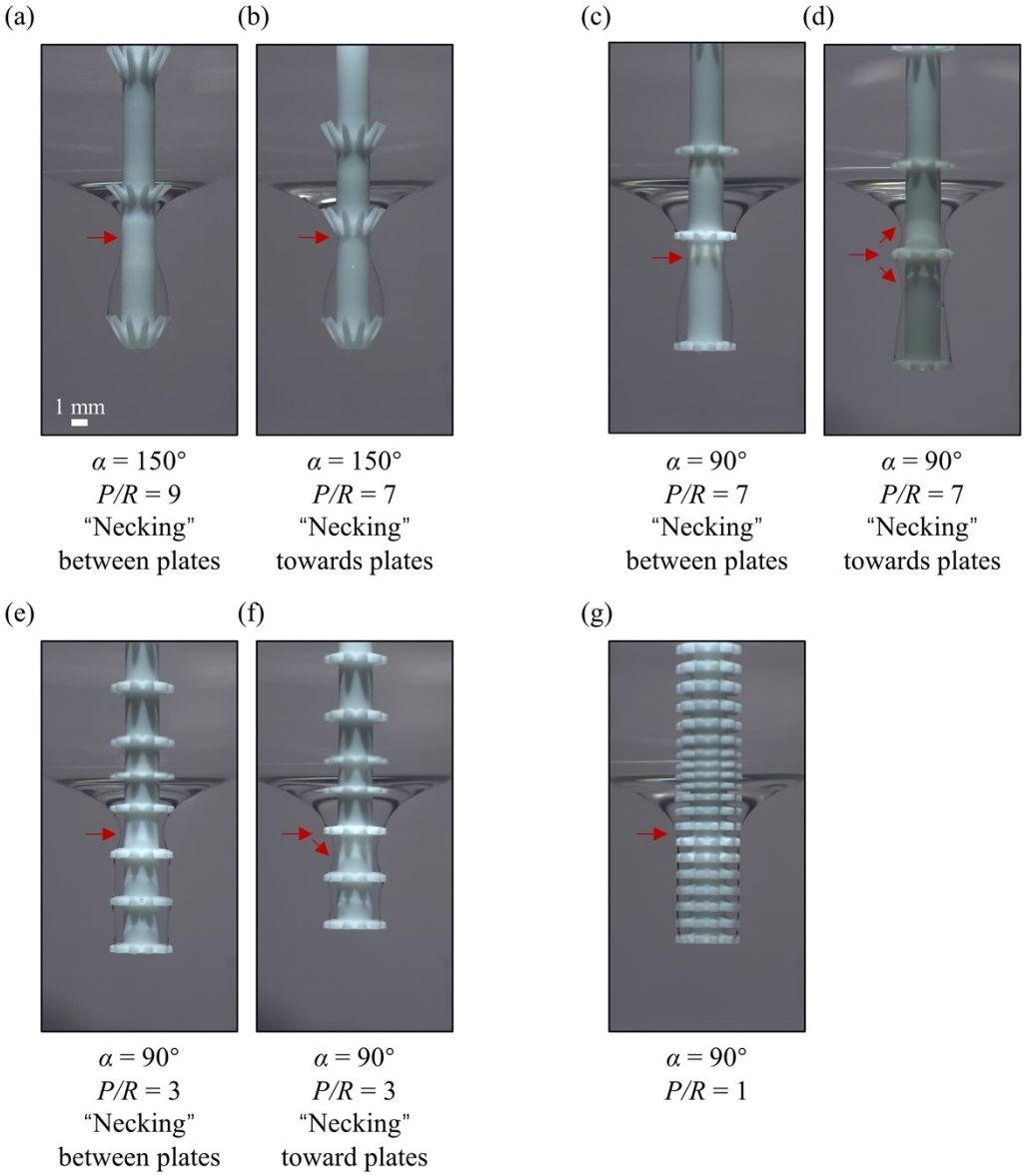

Fig. S4 Optical images at t = 100 s of the plate angle α of (a)-(b) 150° and (c)-(g) 90°, and the dimensionless pitch scale P/R of (a) 9, (b)-(d) 7, (e)-(f) 3, and (g) 1. The immersion deep in (d) was slightly varied to manipulate the relative position of the spiky plate and the "necking" place.

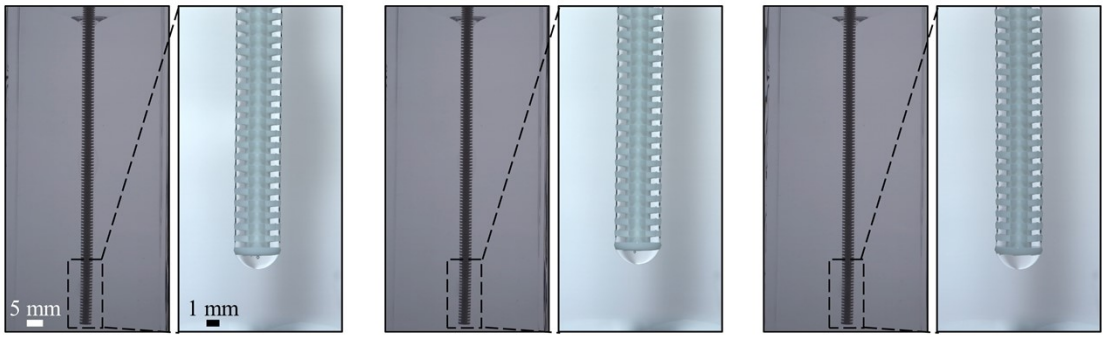

Fig. S5 Optical images of solid object with complete oil film under the depth of 10 cm at t = 1000, 2000, and 3600 s.

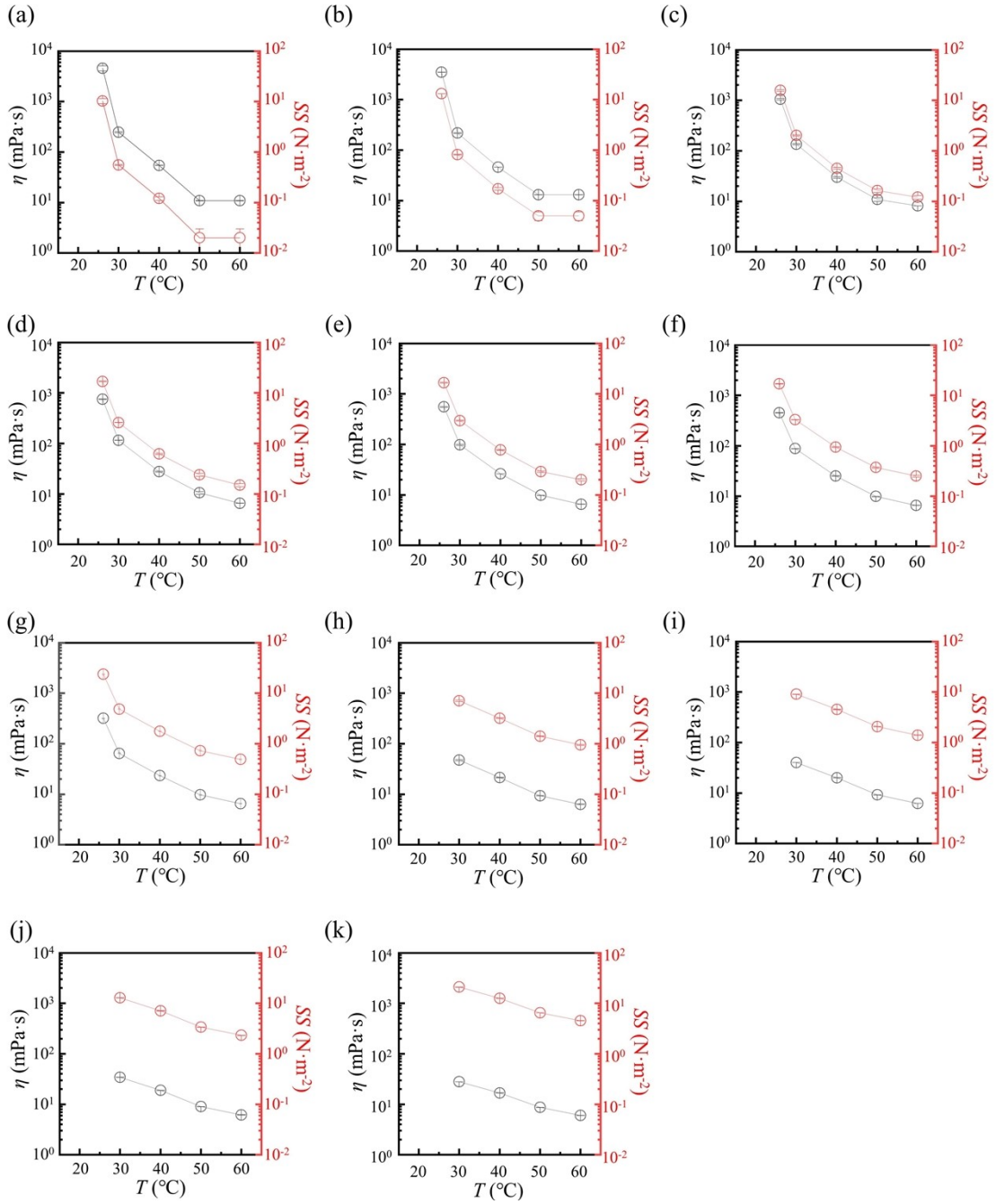

Fig. S6 Viscosity and shear stress of the crude oil at varied temperature. The shear rate here is of (a) 2.25, (b) 3.75, (c) 15.0, (d) 22.5, (e) 30.0, (f) 37.5, (g) 75.0, (h) 150, (i) 225, (j) 375, and (k) 750 s^{-1}. The data are shown as mean ± SD (N = 3), and the error bar represents SD. Note that some errors are smaller than the size of the symbol.

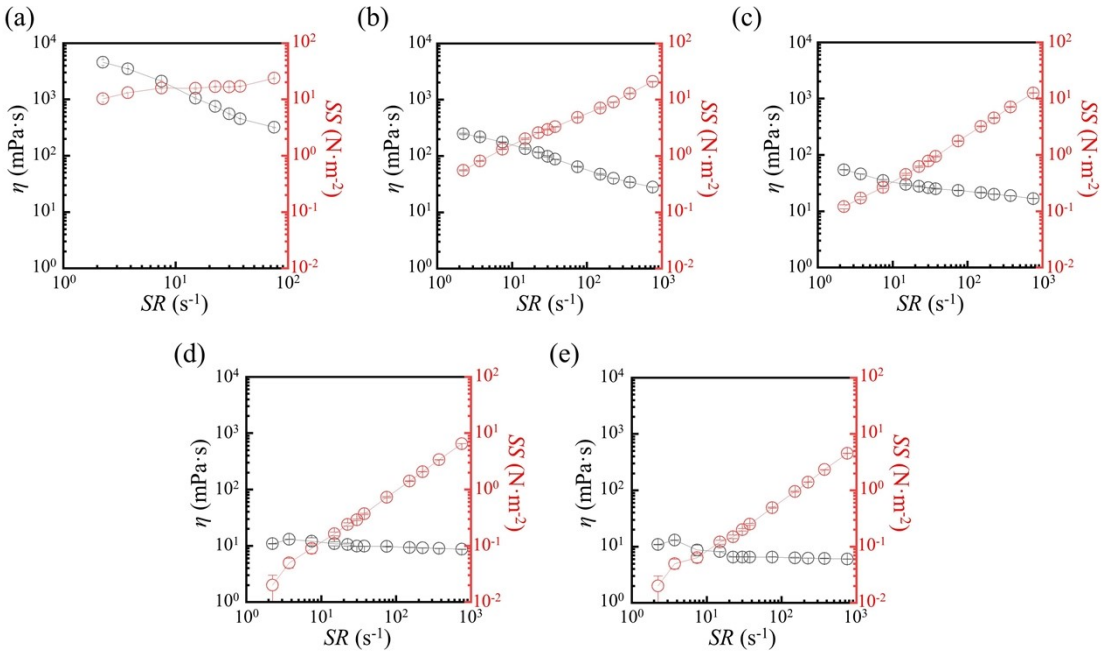

Fig. S7 Viscosity and shear stress of the crude oil at varied shear rate. The temperature is of (a) 26, (b) 30, (c) 40, (d) 50, and (e) 60 °C. The data are shown as mean ± SD (N = 3), and the error bar represents SD. Note that some errors are smaller than the size of the symbol.

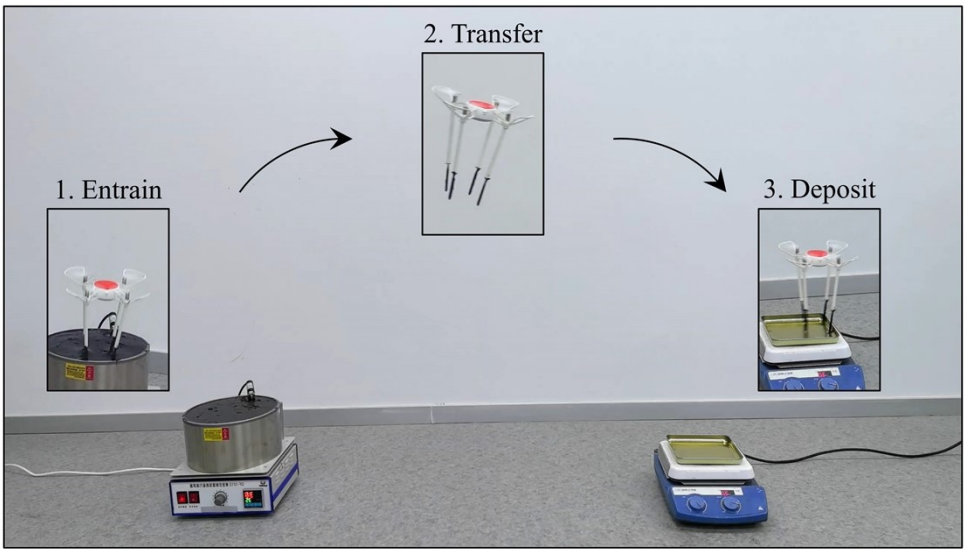

Fig. S8 Typical steps of the floating oil collecting demonstration by a drone equipped with 4 mesoscale-structured objects.

Table S1 Physical properties of silicone oils (SO) used in the experiments. The experimental data are shown as mean ± SD (N = 3). The liquid densities are from the official technical data sheet of the PMX-200 silicone oils.[1]

Liquid	Dynamic viscosity, η (mPa·s)	Density, ρ ($g \cdot mL^{-1}$)	Density difference, $\Delta\rho = \rho_{water}-\rho$ ($g \cdot mL^{-1}$)	Oil-water capillary length, l_c (mm)
SO-10	$(1.11 \pm 0.01) \times 10^1$	0.935	0.065	11.73 ± 0.34
SO-100	$(1.12 \pm 0.02) \times 10^2$	0.964	0.036	11.63 ± 0.57
SO-350	$(3.84 \pm 0.02) \times 10^2$	0.969	0.031	11.66 ± 0.88
SO-1000	$(1.13 \pm 0.02) \times 10^3$	0.970	0.030	11.61 ± 0.74
SO-10000	$(1.02 \pm 0.01) \times 10^4$	0.974	0.026	11.63 ± 0.24

Table S2 Kinematic viscosity ($v = \eta/\rho$) and visco-buoyancy ratio ($\eta/\Delta\rho$) calculated with the data from Table S1.

Liquid	Kinematic viscosity, $v = \eta/\rho$ (cSt)	Visco-buoyancy ratio, $\eta/\Delta\rho$ (cSt)
SO-10	$\approx 1.19 \times 10^1$	$\approx 1.71 \times 10^2$
SO-100	$\approx 1.16 \times 10^2$	$\approx 3.11 \times 10^3$
SO-350	$\approx 3.96 \times 10^2$	$\approx 1.24 \times 10^4$
SO-1000	$\approx 1.16 \times 10^3$	$\approx 3.77 \times 10^4$
SO-10000	$\approx 1.05 \times 10^4$	$\approx 3.92 \times 10^5$

Movie S1 Floating oil collection by the bio-inspired sustained entrainment.

References

1. XIAMETER™ PMX-200 Silicone Fluid, https://www.dow.com/zh-cn/search.html#q=PMX-200%20Silicone%20Fluid&t=All&sort=relevancy, (accessed January 29, 2024).